Carbon Fiber Bicycle Frame Analysis Using Finite Element Modeling

Diogo Ponte Lauda, diogolauda@gmail.com
Maurício Vicente Donadon, donadon@ita.br
ITA Technology Institute of Aeronautics, Pça Mal. do Ar Eduardo Gomes,50 - Vila das Acácias - 12228-900
São José dos Campos - SP

Abstract. *In this work the analysis of a carbon fiber bicycle frame is described. This kind of structure is subjected mainly to dynamic loads, such as impacts from the ground and inertial forces from the cyclist body. The design of a carbon fiber structure adds other variables to the project, as it only makes sense to use carbon fiber to save mass and gain rigidity, which are very dependent on the correct fiber orientation and the matrix choice. By modeling the problem using finite elements on non-linear dynamics analysis it is possible to achieve results very close to the reality and to clearly check the best lay-up schedule and matrix for improving the frame's resistance, weight and rigidity. It was found a standard as a base for loading the structure, which defined two different tests. Those were modeled in commercial software, using contact logic to predict the forces transmitted to the frame from test apparatus and dynamic loads to simulate impacts. The problem was solved using an explicit analysis algorithm. Finally, a stability analysis was done to check the integrity of the structure during the impact. The analysis conclusions permitted building a structure with geometry, material type and orientation defined, with a prediction of weight and safe margins based on international standards.*

Keywords*: bicycle frame, finite element method, composite materials, dynamic analysis.*

1. INTRODUCTION

Different from what is found on a leisure bicycle, the design of a competition frame has some structural challenges, demanding very low weights, since a couple of grams can separate the second for the first place. Structural rigidity has another important hole on those frames: very low rigidity leads to great loses of energy caused by excess of deformation, on the other side, a very high rigidity makes the bike hard to control and uncomfortable, Klein (1985).

The application of composites on sports goods has enabled great developments on recent years. Particularly on cycling industries, carbon fiber reinforced plastic (CFRP) brought lots of advantages due to its properties of great rigidity, low density and great strength, Peters (1997). There is also the possibility to align the fibers adequately, making a structure strong and rigid in some direction that is needed and lass rigid on another, so it can work as an absorber. That is why lots of components in modern bikes are made of CFRP: suspension, wheels, handlebar, seat post, tires, crank arm and frame, among others.

The present paper describes a methodology for analyzing a composite bicycle frame employing the finite element method (FEM). The main objective was to find the distribution of a fail index along the structure, allowing reinforcing only the regions where it was necessary, by changes on the geometry or by local material additions. The load cases were based on specific standards for bicycle safety.

Due to the low weight of the frames nowadays, something around 1 kg, it was necessary to know precisely the stress distribution along the piece, guaranteeing the structural integrity without leading to a weight greater than usual for carbon frames. To make this happen, it was searched a modeling technique which was closest as possible from physical tests and that make possible for a house computer to achieve the convergence on the solution of the dynamic formulation of the problem.

After many consecutive analyses, for each load case, it was found geometry and lay-up schedule that guarantee structural integrity inside the safety margins. The total weight also stands below the maximum established, concluding the analysis objectives.

2. GEOMETRY

The frame geometry comprehends lots of variables to take into account as the impacts on ergonomics, aesthetic appeal, interfaces with other pieces and structural effects. Since this work is only concerned with the structural analysis, the only deem about those aspects in the geometry design for this analysis.

The type of ridding of the bike has a prime importance on its structure, as if defines the intensity and the type of the loads over it. Usually a mountain bike is stronger than a speed one. An downhill frame, in turn, is stronger and heavier than a mountain bike frame. It was decided to analyze a mountain-bike, because this is the most versatile one. The method of analysis could be employed in any other type of frame once the loads are consistently adapted for other values.

The geometry was developed using an commercial CAD software, assuming usual angles for this type of frame. Those usual angles were obtained from comparing geometries of famous bikes suppliers like Giant (2009), Cannondale (2009) and Specialized (2009). Tubes were made with a high diameter, looking for improving the sections inertia

without implying on high weights. Those tubes that would come in contact with the fork and the seat post were made with a compatible diameter.

When the geometry was ready, it was imported for the analysis software using a neutral format (iges).

2. LOADS

Intending to correctly analyze the structure, it was necessary to adopt a standard as a base for the load cases. The ISO 4210 Safety Requirements for Bicycles (1996) was chosen, which states two different tests to be done on frames: the falling mass and the falling frame-fork assembly. In addition to those load cases, it was required that the structure resists the impacts with a margin of 50% based on Tsai-Hill fail index, on each element.

2.1. Falling Mass

On these test, a 22,5 kg mass impacts on the frame-fork assembly, falling from 180 mm to impact a 1 kg mass roller installed in the front of the fork. The assembly is clamped on rear axle attachment points, in a way that a line, passing by both rear and front axles, makes a normal to the ground plane.

After this impact, there shall be no visible evidence of failure, and the permanent deformation of the assembly, measured between the centerlines of the wheel axles, shall not exceed 40mm.

2.2. Falling Frame-Fork Assembly

Using the same assembly for the falling mass test, the second test is done by fixing the rear axle, allowing just rotation on this axle free. A *70 kg* mass must be placed on seat tube, with its center of gravity coincident with this tube center line and on a distance of *75 mm* from the end of it.

The assembly is elevated till the center of gravity of the mass is coincident with a line, perpendicular to the ground, passing through the rear attachment. On this moment, the assembly is allowed to fall, impacting on a steel anvil and concluding the tests.

3. MODELS

During the project, many forms of modeling were employed, starting from simple ones and progressively elevating the sophistication, as it was found important to achieve results closer to the physical reality of the problem.

In this paper it will only be described the final modeling, once it was the most accurate and the one used to determine the final lay-up schedule. This last model predicts the contact between the frame and the other tubes of the assembly: the fork and the seat post tube. The impacts were simulated on a dynamic problem of initial conditions specified by a conservation of energy approach. The solution was obtained through an explicit algorithm, once it was found very difficult to achieve convergence with the implicit one.

The structure was modeled employing around *9000* plate elements, seen in Fig.1, with a refinement degree determined during the analysis based on the precision needed for the results and the computational resources available.

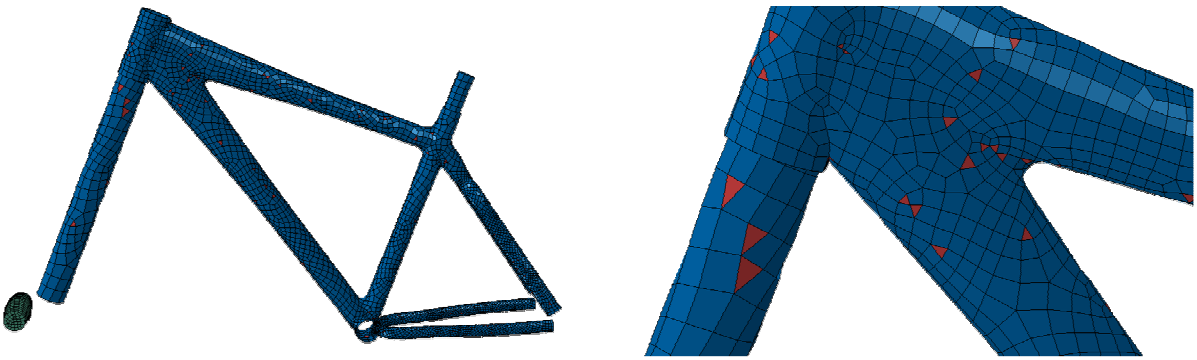

Figure 1: Model representing the frame on ABAQUS. Those elements in blue are S4R, the ones in red are S3R end the green ones are solid tetrahedral TETR.

The properties used to model the carbon fiber laminates was obtained from CENIC Engenharia Ind. Com. Ltda base data, for a T300 unidirectional laminate with epoxy 5052 resign, cured at 80°C and pos-cured at 120°C on a bag molding process. Those properties can be seen on the Tab. 1:

Table 1: Properties of unidirectional carbon fiber with 5052 epoxy resin:

Elastic Properties			Strengths		
E_1	139	GPa	$\sigma_{11,Ut}$	1769	MPa
E_2	9,21	GPa	$\sigma_{22,Ut}$	52,1	MPa
$G_{12}=G_{13}$	5,39	GPa	τ_{12}	102	MPa
G_{23}	3,542	GPa	$\sigma_{11,Uc}$	1037	MPa
$v_{12}=v_{13}$	0,32		$\sigma_{22,Uc}$	199	MPa
v_{21}	0,024				
v_{23}	0,3		Density	1600	$Kg.m^{-3}$

The 1 axis is the laminate principal axis, which means that in a 0° unidirectional composite the 1 axis will be coincident with the fibers direction. The 3 axis is normal to the laminas plane and the 2 axis completes the trihedral coordinate system.

E_x – Is the Young's Modulus of the x axis of the lamina;
G_{xy} – Represents the Shear modulus on the xy plane;
v_{xy} – Represents the Poisson ratio's in the xy plane;
$\sigma_{xx,Ut}$ – Represents the ultimate stress in traction in the x-axis;
$\sigma_{xx,Uc}$ – Represents the ultimate stress in compression in the x-axis;
τ_{12} – Represents the ultimate shear in 12 plane;

To determine the orientation of the laminate main axis, the symmetry axis of the tubes was used as reference. It is important to notice that the transition region between different tubes leads to a discontinuity of properties, since the modeling of a smooth transition would make necessary the definition of different axis for each element in the region, a task that would demand an immense effort of time. Then, it is expected to find a numeric discontinuity on the stress field on these regions that would not be present in a real situation.

The other pieces that come in contact with the frame were modeled using the properties of the AISI 1025 Steel and the AL 6061 aluminum, which can be find on Tab. 2 and Tab. 3 above, obtained from MIL-HDBK-5J (2003). The fork tube and the seat post tube were made of aluminum and with plate elements. The rolling mass was simulated using the steel properties and tetrahedral solid elements.

Table 1: Properties of Al-6061 T651 aluminum, extracted from MIL-HDBK 5J:

Al- 6061 Properties		
E	71	GPa
G	26	GPa
v	0,33	
Density	2700	$Kg.m^{-3}$

Table 2: Properties of AISI 1025 steel extracted from MIL-HDBK 5:5:

AISI 1025 Properties		
E	200	GPa
G	76	GPa
v	0,3	
Density	7861	$Kg.m^{-3}$

Since metals where considered as isotropic materials, there is no need to use subscripts to identify materials axis for the engineering constants.

3.1. Case 1: Falling Mass

To adapt the model for the falling mass test it was necessary to clamp the rear attachment and then to add a concentrated mass on the roller, with the value of *22,5 kg*. Over this mass was imposed a *1,9 m/s* initial condition, obtained by the conversion of gravitational potential energy to kinetic energy just before the impact:

$$E_P = mgh = E_C = \frac{mv^2}{2} \tag{1}$$

Where *h* is the variation of the vertical component of the impact mass, from the initial to the final position, when it hits the frame.

Although this modeling technique does not represent exactly what really happens during the impact, the results along the first impact are very close. This occurs because during the real impact test the mass maintains constant contact with the roller, as it decelerates, converting kinetic energy into elastic potential energy plus a small energy fraction dissipated as heat. After the mass complete stop, the frame will star releasing the stored energy, pushing the mass upright till the equilibrium position, when the contact stops. Until this final contact instant, simulating the *22,5 kg* mass by a concentrated one fixed on the roller it's a good approximation due to the constant contact explained above. It is important to notice that after this moment this modeling is no longer valid. Since the first impact is the most critical one, if the model resists it will certainly resist the others.

As the structural damping was very difficult to know without experiments, it was neglected in a conservative approach. This happens since any kinetic energy turns to be dissipated during the impact, leading to more energy being stored as elastic potential energy, which leads to higher stress levels.

3.1.1 Results

On Fig. 2 below, it can be seen on the color scale the most critical frame step along the impact, based on Tsai-Hill criteria. The tubes representing the frame fork and the seat-post tube are seen in white elements, with no color scale, since there is any interest in analyzing those components in this work.

On the composites elements, the failure indexes were very low, in general, and the higher values were found on tubes transition regions.

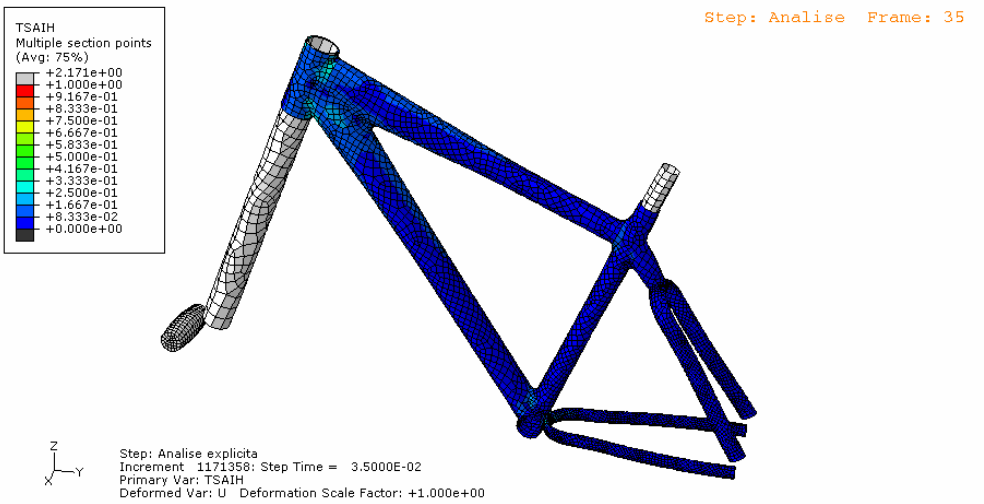

Figure 2: Tsai-Hill plotting along the model. Time STEP $3{,}5.10^{-2}$, Biggest Tsai-Hill index = 2,171.

Zooming the inferior region of the head tube, it can be seen that some elements fail. On the color scale it is indicated a maximum failure index value of 2,171. These types of transition regions would require a more sophisticated modeling, with a greater refinement and absence of discontinuities between the elements, in order to correctly predict the failure characteristic.

Since this failure is localized, it was considered unnecessary to reinforce the region and, instead of it, adding aluminum ring when building the prototype to the structural tests.

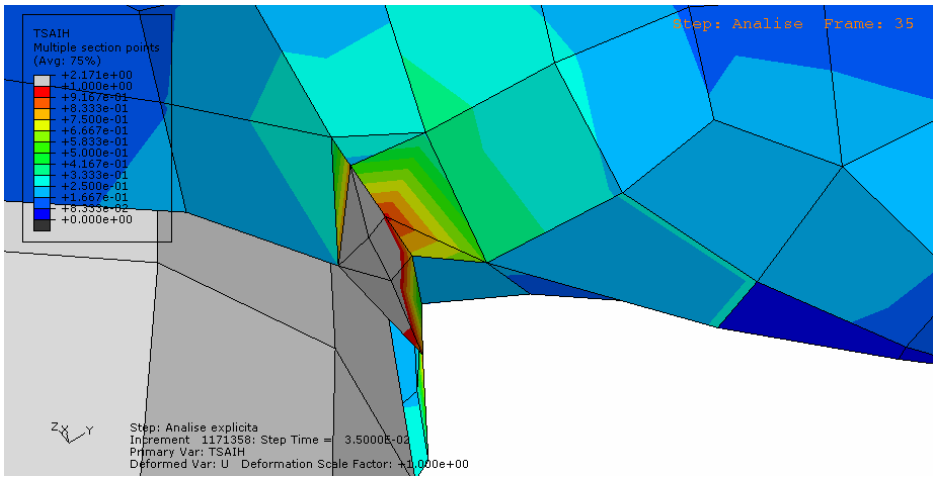

Figure 3: Elements that indicate failure on the bottom of head tube.

3.2. Case 2: Falling Frame Fork Assembly

Based on the final model that passed case 1, it proceeded with the modeling of the second one. It was done by setting just one degree of freedom on the rear attachments of the frame, allowing the rotation on the rear axle. The concentrated mass was removed from de rolling mass, and another one placed on the position established by the standard and with the value of *70 kg*.

The rolling mass was restrained to translate perpendicular to the impact plane. This condition represents the moment that the rolling mass hits the steel anvil, and starts to slide over it. By simulating the problem like this turns it more conservative, once that constrain will work as a plane with infinite rigidity, and will make much easier to achieve the convergence on the analysis.

The velocity on the moment of impact was imposed as an initial condition for the dynamic problem, in the form of angular velocity distributed on all model in respect to the rear axle. To obtain this velocity conservation of energy was applied again, this time with the conversion of gravitational potential energy into rotational kinetic energy:

$$E_r = \frac{I\dot{\theta}^2}{2} \tag{2}$$

$$E_p = mgh \tag{3}$$

$$E_p = E_r \tag{4}$$

The assembly inertia´s, Eq. (2) was easily obtained from the software. The variation of high *h*, Eq. (7) was obtained from the assembly´s center of gravity vertical component. The same was done to obtain the weight, Eq. (6).

$$I = (19.08)\ m^2 kg \tag{5}$$

$$m = (72.4)\ kg \tag{6}$$

$$h = (0{,}0323)\ m \tag{7}$$

This leads to the following value, Eq. (8), for the rotational velocity of the assembly:

$$w = (1{,}55)\ rad/s \tag{8}$$

The model is depicted in fig. 4:

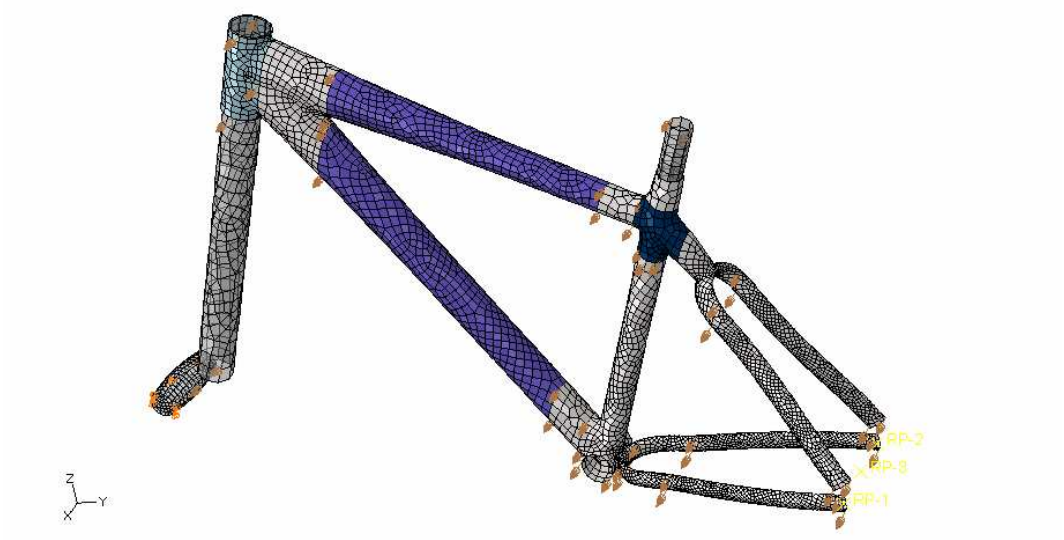

Figure 4: Model representing the second test with different colors representing different laminate regions.

3.2.1 Results

Again the highest failure index values were found on the tubes transitions regions. On fig. 5 a close of the head tube is shown. Except for local stress concentrations, the biggest values were found around 0,6. On the head tube´s top portion a small red region is seen, indicating the failure. The same way as explained before it was decided to add a local reinforcement and check on the physical tests.

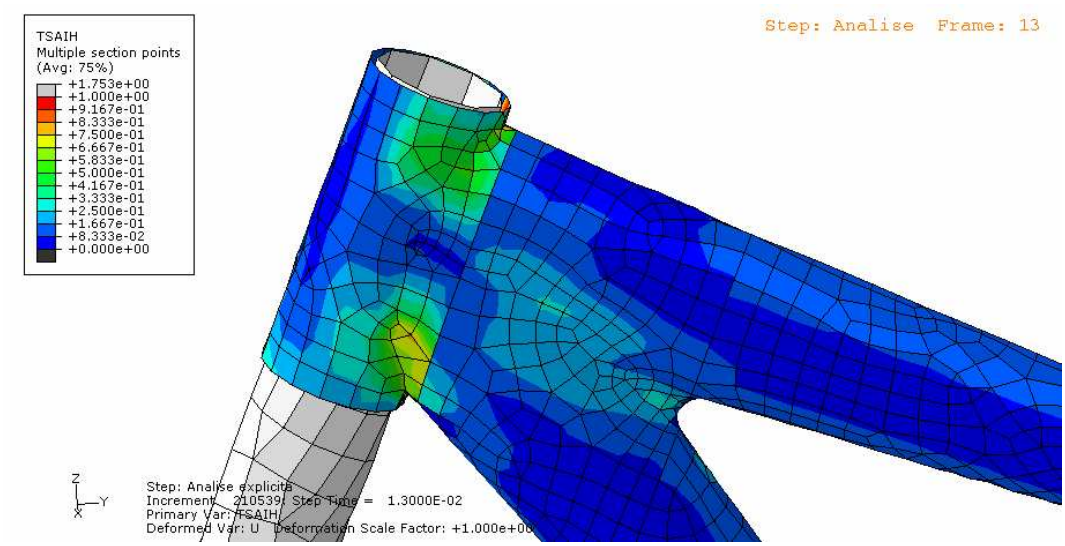

Figure 5: Head tube Tsai-Hill fail index plotting for the second test.

On fig. 6 the seat tube is seen in detail. This portion was found to be another critical region of the frame in this test since it resists a very strong flexural moment. With the final lay-up schedule the biggest failure index in this region was 0,66 indicating no failure.

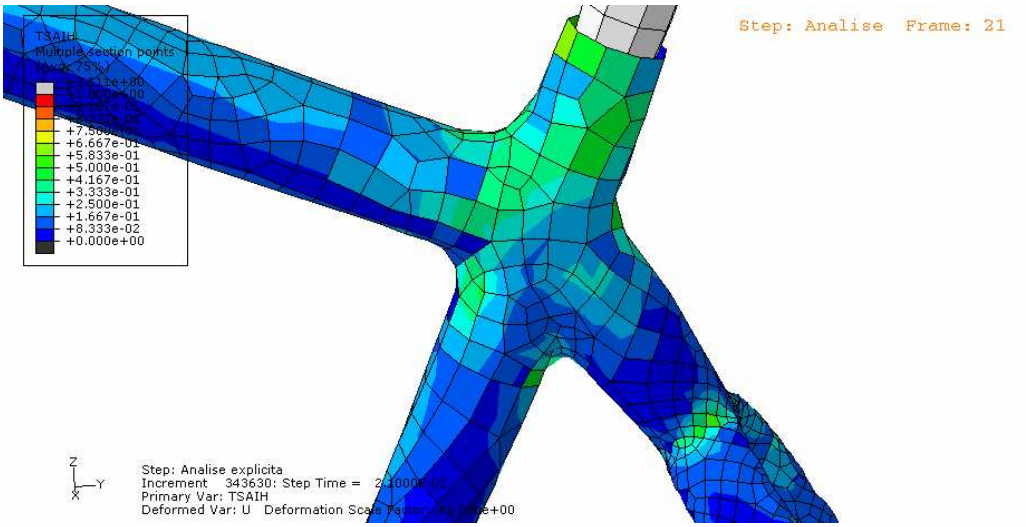

Figure 6: Fail index on seat tube for the second test.

The last critical region was the bottom bracket tube, which can be seen detailed on fig. 7. The connection elements between the chain stays and the bottom bracket tube indicate failure. Modeling this kind of region is really hard since the main axis of the laminate should be defined for each element. In addition to this the elements sizes should be very small due to the low curvature radius in this portion. Those results points to a stress concentrations that probably won´t exist on the real frame. A local reinforcement was established and the failure analysis concluded.

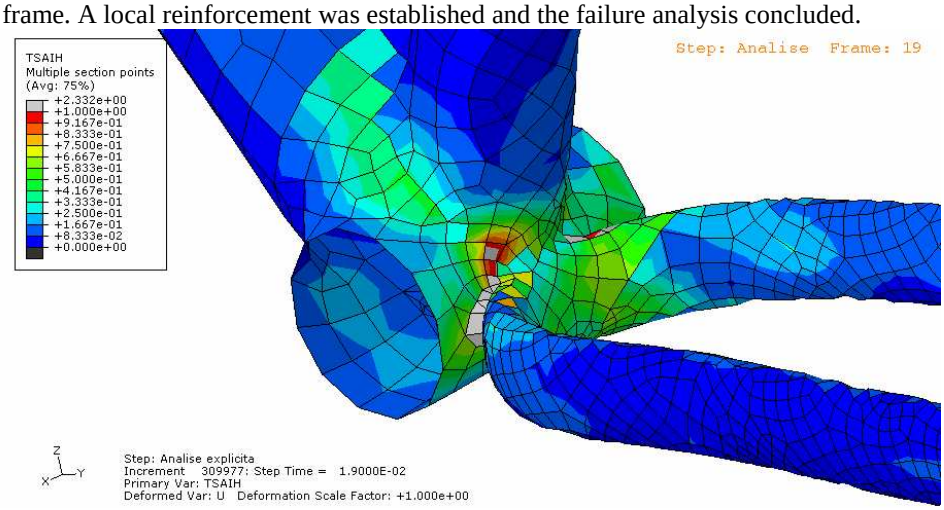

Figure 7: Fail index around the bottom bracket in second test.

3.3. Stability analysis

To make sure that the frame would pass on posteriors test, if was found necessary to check the model stability since some sections were made very thin what can lead to local buckle. The same tests described above were modeled again, but know directed to buckle. The problem was modeled on FEMAP, and solved with NX NASTRAN, comprehending 3166 plate elements, manly QUAD.

Models constrains where made in the same way as before. The unitary force load on the first case was defined in the same direction as the velocity initial condition was on the dynamic model.

On the second, the unitary force load was positioned over the CG of the 70 kg mass, since it is 97% of the total, and was aligned to the tangential velocity the mass would have just before the impact.

This approach is explained from the dynamic nature of the loads over the frame. When the frame is impacted, the deceleration of the masses transmits great forces to the structure. By checking buckle on the frame with forces on the same direction of the deceleration of the masses, it is possible to discover at which value this would happen. Then, since the duration of the impact is known from the dynamic analysis, it is possible to predict the forces acting during the shock from impulse theorem and, consequently, if occurs buckle or not.

The time for stopping the mass on first simulation was $3{,}5.10^{-2}$ seconds. With a *22,5 kg* mass and initial velocity of *1,9 m/s*, the average force acting during the shock was:

$$F_{Test1} = 1221\ N \tag{9}$$

For the second test, the time for sopping was $1{,}4.10^{-2}$ seconds, with a *70 kg* mass and an initial velocity of *1 m/s*, the average force acting on second test was:

$$F_{Test2} = 5000\ N \tag{10}$$

The analysis results, Fig. 8 for the first test indicate a first buckle with *11319,45 N* of force acting over the frame. This value is much higher than expected for this test, indicating that the frame is stable on the first case.

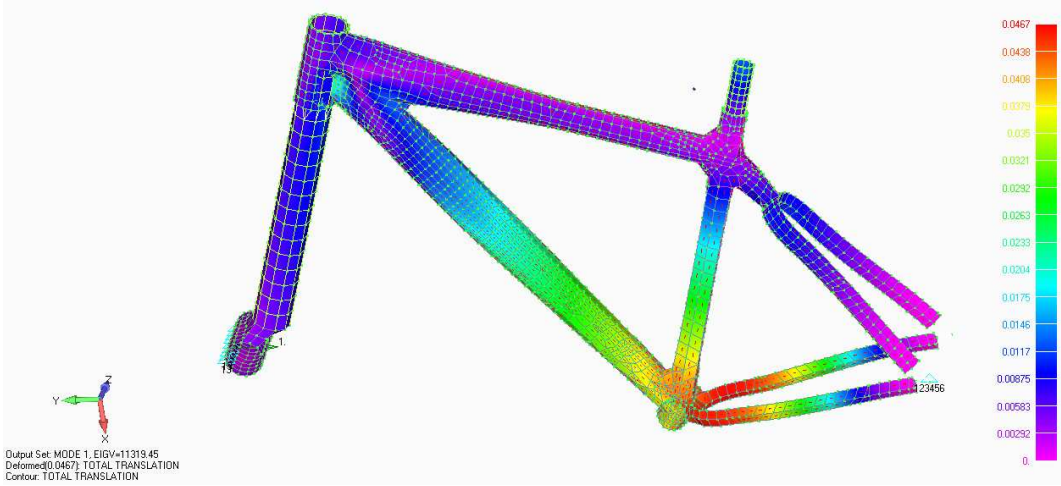

Figura 8: First mode of buckle for the Falling Mass Test (11319,45 N). Color scale plotting translations over the frame.

On the second analysis the first buckle mode happens with a force of 20683,5 N, in a anti-symmetrical mode, seen on Fig. 9 above. Comparing this value with the estimated average force for this test, there is no buckle expected.

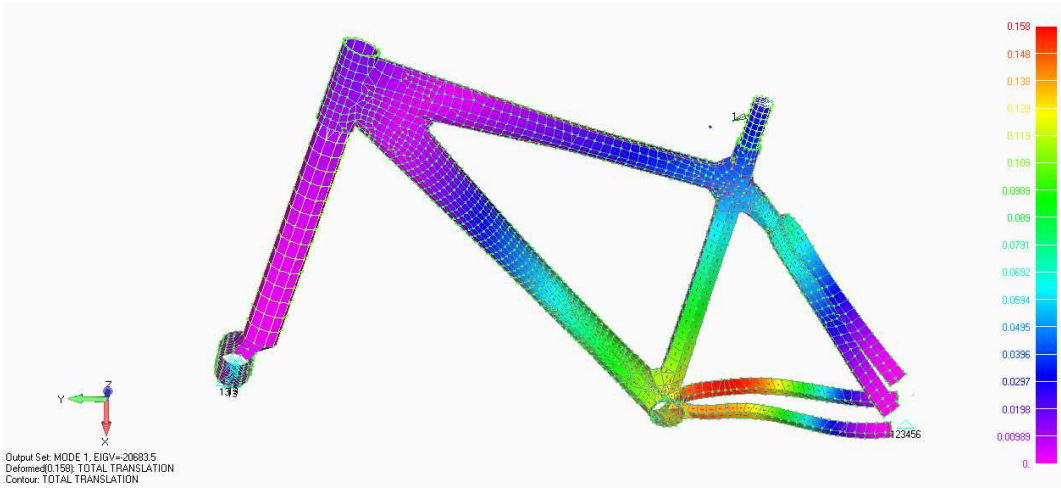

Figure 9: First buckle at 20683N. Color scale indicating of translation over the frame.

4. CONCLUSIONS

The results of those simulations indicate that the frame won't fail, once the lay-up schedule is used as defined in the analysis. Information on the lay-up definition along the structure and the amount of material defined through the simulations presented in this paper are confidential.

The total weight of the structure was estimated to be around *780 g*, a reasonable weight for the structural mass. In the production process there will always be some additional weight due to excess of materials as resin and fibers. There is also the inserts that are necessary to enable interfaces between the frame and the other pieces. Taking everything into account to total weight will rest around *1,1 kg*, a very light frame for mountain bikes.

The method of analysis described above can be used for any kind of frame by adjusting the margin of safety according to the use of the frame: a downhill application will require much more from the frame when compared to a speed bike, which makes important to guarantee higher margins or to raise the loads by an adequate factor.

It was not calculated any prediction of structural rigidity of the frame in the method. This can lead to a very rigid or very soft frame, both inefficient. Thus, the method can guarantee a safe structure but, in other to completely design a competition frame, it will be necessary additional efforts to achieve a lay-up schedule with an adequate rigidity.

5. REFERENCES

Cannondale, 2009. Moutain Bikes.
<http://www.cannondale.com/usa/usaeng/Products/Bikes/Mountain/>

Department of Defense, United States of America, 2003. "MIL Handbook 5J - Metallic Materials and Elements for Aerospace Vehicle Structures".

Giant-Bicycles, 2009. Off Road Bikes.
<http://www.giant-bicycles.com/en-US/bike-finder/everyone/offroad/?level=all>

ISO International Standard, 1996. "Cycles – Safety requirements for Bicycles".

Klein, Gary G., 19 de Fevereiro de 1985. "High Efficiency Bicycle Frame", United States Patent Nº4,500,103

Peters, S. T.,1997. "Handbook of Composites", 2 Ed. Charpman e Hall.

Specialized, 2009. Mountain Bikes.
< http://www.specialized.com/us/en/bc/SBCMain.jsp?scid=1000>

6. RESPONSIBILITY NOTICE

The author(s) is (are) the only responsible for the printed material included in this paper.